Inelastic Response of Ring-Stiffened Cylindrical Shells to External Pressure Shock Waves

L. H. N. Lee* and J. T. Horng†
University of Notre Dame, Notre Dame, Ind.

An incremental finite-differences approach based on an absolute minimum principle in dynamic finite plasticity is developed to study the inelastic response of ring-stiffened cylindrical shells to external pressure shock waves. The pressure in the shock wave is treated as a prescribed transient load. Numerical results for five cases are presented. The results indicate that dynamic stress concentrations and yielding occur in a shell near the ring stiffeners or other hard points.

Introduction

THE purpose of this investigation is to determine the inelastic response of ring-stiffened cylindrical shells to shock loads such as that produced by atmospheric or underwater explosions. An excellent introductory account of underwater explosions has been given by Cole.[1] The physical processes initiated by an underwater explosion consist of a chemical reaction in the explosive, the development and thermal expansion of a gas sphere, the propagation of spherical shock waves in the water, and surface effects. With the presence of a submerged structure, the pressures developed by the explosion both affect and are affected by the structure. The interactions between the fluids and solid, in the forms of transmission, refraction and reflection waves in the media, cavitation and turbulent flow, and deformation and motion of the structure, are indeed very complex. Up to now, only the linear interactions between elastic cylindrical shells and inviscid fluids under simple or uniform loading conditions has been studied.[2-10]

In this paper, no attempt is made to analyze the nonlinear, inelastic fluid-solid interactions. The impulse of a shock wave acting on a cylindrical shell is assumed to be in the form of a prescribed pressure distribution as a function of the radial distance from a center of explosion and time, such as that occurred in an underwater explosion without the presence of a submerged structure. It is also assumed that the center of explosion is sufficiently distant from the shell such that the peak pressure in the incident wave is relatively moderate and the stresses normal to the middle surface of the shell are relatively small. In other words, the effects of wave propagation through the thickness of the shell on its yielding may be ignored. Furthermore, Love-Kirchhoff assumptions for a thin shell subject to displacements of an order of the thickness and small strains are employed in the analysis.

To obtain a solution of the problem, a variational approach based on an absolute minimum principle in dynamics of elastic-plastic continua at finite deformation[11] is employed. The minimum principle is based on the concept of employing finite differences in accelerations in formulating a variational principle as depicted by Gibbs in classical mechanics.[12] The concept is most suitable for treating nonholonomic problems. The method of finite differences by Euler, a direct method of variational calculus, is employed in a timewise step-by-step integration procedure to obtain the numerical results in the paper.

Received March 21, 1975; revision received Oct. 3, 1975. The research was sponsored by the Office of Naval Research under Contract N00014-0152 to the University of Notre Dame.

Index categories: Structural Dynamic Analysis; Shock Waves and Detonations; Marine Vessel Design.

*Professor, Department of Aerospace and Mechanical Engineering.
†Research Assistant, Engineering Science Program.

Minimum Principle

Consider a body of a continuum occupying in its natural state a region V_0 and bounded by a surface A. The body is subjected to time-dependent body force F_M (per unit mass) and Lagrangian surface traction (per unit initial area) T_M over that part of the initial surface area A_T. At time t, let $\{U_K\}$ be the displacement vector of a particle of the body which has an initial position of $\{X_K\}$ in a curvilinear coordinate system. The displacements are prescribed over that part of the boundary surface A_U. The deformation of the body may be described in terms of the covariant components of the Lagrangian strain tensor E_{KL} defined by

$$E_{KL} = \tfrac{1}{2}(U_{K;L} + U_{L;K} + U^M{}_{;K} \cdot U_{M;L}) \tag{1}$$

Herein, a covariant derivative of a variable with respect to X_K is designated as $(\ )_{;K}$. The Lagrangian strain may be expressed as the sum of two parts: elastic strain E'_{KL} and plastic strain E''_{KL}. It is postulated that the constitutive relationships, in terms of the symmetric Kirchhoff stress tensor S_{KL}, may be strain-velocity dependent such as

$$S_{KL} = S_{KL}(E'_{MN}, E''_{MN}, \dot{E}''_{MN}, \kappa, \Theta) \tag{2}$$

in which Θ is the temperature and $\dot{E}''_{MN}$ is the velocity rate of plastic straining. In Eq. (2), κ is a work-hardening parameter which depends on the history of plastic deformation. The contravariant components of the Kirchhoff stress tensor S^{KL} satisfy the boundary conditions

$$S^{KL}(g_{ML} + U_{M;L})N_K = T_M \text{ on } A_T \tag{3}$$

in which N_K is the covariant outward unit normal to A, and g_{ML} is the metric tensor.

It has been shown[11] that the true acceleration field, $\ddot{U}_M = D^2U_M/Dt^2$, of the body, which has known or predetermined displacement and velocity fields at time t, is distinguished from all kinematically admissible ones by having the minimum value of the following functional

$$I = \int_{V_0} S^{KL}\ddot{E}_{KL}\,dV_0 + \frac{1}{2}\int_{V_0} \rho_0\ddot{U}_M^2\,dV_0 - \int_{A_T} T^M\ddot{U}_M\,dA - \int_{V_0} \rho_0 F^M\ddot{U}_M\,dV_0 \tag{4}$$

in which ρ_0 is the initial mass density. The minimum principle is valid for continuous as well as sectionally discontinuous acceleration fields. Ordinarily, it is sufficient to use the first variation with respect to the acceleration, $\delta_{acc}I = 0$, to establish governing equations or to solve a problem by a direct method of variational calculus.

Kinematics

Consider a cylindrical shell of mean radius a, thickness h, and axial length L. The shell is stiffened by N equally spaced, internal rings of a rectangular cross section of width b and depth d shown in Fig. 1. Let $(\bar{x}, \theta, \bar{z})$ be the axial, circumferential, and (inward) normal coordinates and let (U_x, U_θ, U_z) be the corresponding physical components of the displacement vector of a point in the shell, respectively. It is assumed that the deformation of the shell is such that the rotation of an element anywhere in the shell is relatively small (less than 15°) and the change in thickness is negligible. Furthermore, by utilizing Love-Kirchhoff assumptions for thin shells and by omitting wave propagations through the thickness of the shell, the displacements of any particle may be expressed in terms of the corresponding displacements and their derivatives at the middle surface such as

$$\begin{aligned} U_x &= \bar{u} - \bar{z}\bar{w}_{,\bar{x}} \\ U_\theta &= \bar{v} - \frac{\bar{z}}{a}(\bar{w}_{,\theta} + \bar{v}) \\ U_z &= \bar{w} \end{aligned} \tag{5}$$

where $\bar{u}$, $\bar{v}$, and $\bar{w}$ denote the axial, tangential, and (inward) normal displacement components of a point at the middle surface, respectively.

To simplify the subsequent derivations, the following nondimensional quantities are introduced:

$$x = \frac{\bar{x}}{a}, \quad z = \frac{\bar{z}}{a}, \quad U = \frac{\bar{u}}{a}, \quad v = \frac{\bar{v}}{a}, \quad w = \frac{\bar{w}}{a}, \quad w_{,x} = \frac{\partial w}{\partial x} \tag{6}$$

Substituting Eqs. (6) into Eq. (1) and taking the covariant derivatives and time derivatives of the Lagrangian strain tensor, the following strain-accelerations are found:

$$\ddot{E}_{xx} = (1+u_{,x})u_{,x} + v_{,x}\ddot{v}_{,x} + w_{,x}\ddot{w}_{,x} - z\ddot{w}_{,xx} + \dot{u}^2{}_{,x} + \dot{v}^2{}_{,x} + \dot{w}^2{}_{,x} \tag{7a}$$

$$\begin{aligned} \ddot{E}_{x\theta} = \frac{1}{2}\,[&u_{,\theta}\ddot{u}_{,x} + (1+v_{,\theta}-w)\ddot{v}_{,x} + (v+w_{,\theta})\ddot{w}_{,x} \\ &+ (1+u_{,x})\ddot{u}_{,\theta} + v_{,x}(\ddot{v}_{,\theta} - \ddot{w}) + w_{,x}(\ddot{v} + \ddot{w}_{,\theta}) \\ &- z(2\ddot{w}_{,x\theta} + \ddot{v}_{,x}) + \dot{u}_{,x}\dot{u}_{,\theta} + \dot{v}_{,x}(\dot{v}_{,\theta} - \dot{w}) + \dot{w}_{,x}(\dot{v} + \dot{w}_{,\theta}) \end{aligned} \tag{7b}$$

$$\ddot{E}_{\theta\theta} = u_{,\theta}\ddot{u}_{,\theta} + (1+v_{,\theta}-w)(\ddot{v}_{,\theta} - \ddot{w}) + (v+w_{,\theta})(\ddot{w}_{,\theta} + \ddot{v}) - z(\ddot{w}_{,\theta\theta} + \ddot{v}_{,\theta}) + \dot{u}^2_{,\theta} + (\dot{v}_{,\theta} - \dot{w})^2 + (\dot{v} + \dot{w}_{,\theta})^2 \tag{7c}$$

As shown in Fig. 1, the center of explosion is assumed to be in the plane of symmetry of the shell and the ends of the shell are capped with two rigid end plates simulating bulkheads. The symmetric conditions as shown in Fig. 2, permit an end plate to have only axial and transverse displacements, $\bar{U}(t)$ and $\bar{V}(t)$, respectively, and a rigid rotation through an angle $\phi(t)$ about the vertical axis. By assuming that ϕ is relatively small, the dimensionless middle-surface displacements of the shell at the end may be expressed as

$$\begin{aligned} u &= U - \phi\cos\theta \\ v &= V\sin\theta \\ w &= V\cos\theta \quad \text{at } x = \frac{L}{2a} \end{aligned} \tag{8}$$

where $U = \bar{U}/a$ and $V = -V/a$ are dimensionless end displacements. Furthermore, additional boundary conditions are

$$\begin{aligned} v_{,x} &= -\phi\sin\theta \\ w_{,x} &= -\phi\cos\theta \\ v_{,\theta} &= -V\cos\theta \end{aligned}$$

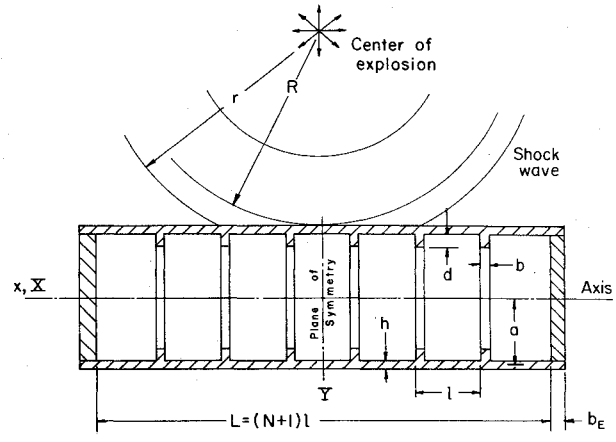

Fig. 1 Shell geometry.

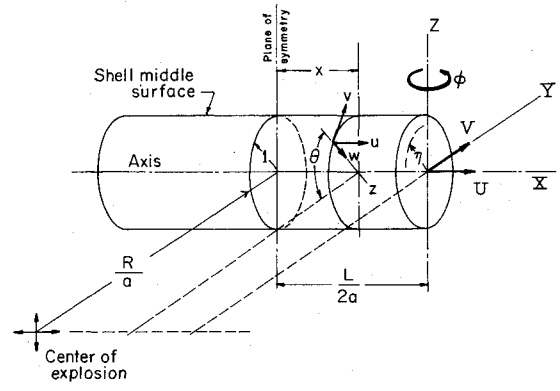

Fig. 2 Dimensionless shell displacements.

and

$$w_{,\theta} = -V\sin\theta \quad \text{at } x = \frac{L}{2a} \tag{9}$$

At the plane of symmetry of the shell, at any time, the middle-surface displacement must satisfy the following symmetry conditions:

$$u = v_{,x} = w_{,x} = 0 \quad \text{at } x = 0$$

and

$$v = v_{,\theta} = w_{,\theta} = 0 \text{ at } x = 0 \text{ and } \theta = 0, \pi \tag{10}$$

Stress-Strain Relationships

It is assumed that the shell material is isotropic and homogeneous and has an elastic stress-strain relationship given by

$$\dot{E}'_{KL} = \frac{1}{E}\,[(1+\nu)\dot{S}_{KL} - \nu\delta_{KL}\dot{S}_{MM}] \tag{11}$$

where E is Young's modulus of elasticity, ν Poisson's ratio, and δ_{KL} the Kronecker symbol. The plastic stress-strain relationship follows that of the classical simple flow theory of plasticity, von Mises J_2 yield surface and isotropic hardening rule.

The rate of hardening may be derived from the uniaxial stress (S) versus strain (ϵ) relationship given by the following Ramberg-Osgood description.[13]

$$\epsilon = \frac{S}{E}\left[1 + \frac{3}{7}\left[\frac{S}{F_{,7}}\right]^{\lambda-1}\right] \tag{12}$$

where $F_{.7}$ is the secant stress intersected by the line $S=0.7E\epsilon$ and λ is a shape factor.

Shock Wave Pressure

The transient pressure p in the units of psi, at a point in the water accompanying the passage of a shock wave, for instance, caused by the explosion of a TNT charge of a weight of W pounds, may be approximately determined by the following semiempirical formula given by Cole:[1]

$$p(r,t)=2.16\times 10^4\cdot\left[\frac{W^{1/3}}{r}\right]^{1.13}H(\tau)e^{-(t-\tau)/\gamma} \quad (13)$$

where r is the distance, in feet, of the point from the center of explosion, $H(\tau)$ Heaviside unit step function, and τ the time of arrival, in seconds, of the shock front. The quantity γ is a decay time constant given by

$$\gamma=0.7676\times 10^{-5}W^{1/3}\left[\frac{r}{W^{1/3}}\right]^{0.24}\text{sec} \quad (14)$$

The strength of the explosion may be described in terms of the shock factor F, defined by

$$F=W^{1/3}/R \quad (15)$$

where R is the distance between the center of explosion and the point $(\bar{x}=0,\ \theta=0,\ \bar{z}=-h/2)$ in the shell. The rate of propagation of shock wave is pressure dependent but decreases rapidly to the speed of sound of about 4900 ft/sec in sea water (at 18° Centigrade). It is assumed that the shell is in a region where the speed of the shock wave C_0 is approximately the speed of sound. Therefore, the time of arrival of the shock front may be determined by

$$\tau=(r-R)/C_0 \quad (16)$$

The Lagrangian surface traction, T_M in Eq. (3), is related to the pressure loading by the equation

$$T_M dA=-p\delta_M^k n_k da \quad (17)$$

where dA is the initial area element, da the corresponding deformed area element, $\delta_M^k$the shifter, and $n_k$the unit normal of da. When the displacements are relatively small, the traction may be simplified to

$$T_K=-p[N_K+N_K U_{;M}^M+N_M U_{;K}^M] \quad (18)$$

Method of Solution

For the ring-stiffened cylindrical shell, the functional I in Eq. (4) may now be specialized to the form

$$\begin{aligned}I=4a^3&\int_0^{L/2a}\int_0^{\pi}\int_{-h/2a}^{h/2a}(S_{xx}\ddot{E}_{xx}\\&+2S_{x\theta}\ddot{E}_{x\theta}+S_{\theta\theta})\,dx\,d\theta\,dz\\&+4a^2b\sum_{\text{rings}}\int_0^{\pi}\int_{h/2a}^{h/2a}S_{\theta\theta}\ddot{E}_{\theta\theta}\,d\theta\,dz\\&+2\rho_0a^4h\int_0^{L/2a}\int_0^{\pi}(\ddot{u}^2+\ddot{v}^2+\ddot{w}^2)\,dx\,d\theta\\&+2\rho_0a^3bd\sum_{\text{rings}}\int_0^{\pi}(\ddot{u}^2+\ddot{v}^2+\ddot{w}^2)\,d\theta\\&-4a^3\int_0^{L/2a}\int_0^{\pi}p\{[1+u_{,x}+v_{,\theta}-\frac{h}{2a}(w_{,xx}+w_{,\theta\theta}+v_{,\theta})]\ddot{w}\\&-w_{,x}(\ddot{u}-\frac{h}{2a}\ddot{w}_{,x})-w_{,\theta}[\ddot{v}-\frac{h}{2a}(\ddot{w}_{,\theta}+\ddot{v})]\}\,dx\,d\theta\\&+2\pi\rho_E b_E a^2\left[a+\frac{h}{2}\right]^2(\ddot{U}^2+\ddot{V}^2+\frac{1}{2}\ddot{\phi}^2)\\&+4a^3\int_0^{1+h/2a}\int_0^{\pi}p[(1+V\cos\theta)\ddot{U}\\&+\phi(\cos^2\theta-\eta\sin^2\theta)\ddot{V}-\eta\cos\theta(1+V\cos\theta)\ddot{\phi}]\eta\,d\eta\,d\theta \quad (19)\end{aligned}$$

where ρ_E is the mass density and η a dimensionless radial coordinate of the end plate. In Eq. (19), it is assumed that the rings are subjected to circumferential stresses only and that the rotational inertias of the shell and rings are negligible.

In Eq. (19), the spatial derivatives of accelerations and displacements are replaced by discrete values of accelerations and middle-surface displacements $(u_{ij},\ v_{ij},\ w_{ij})$ through a finite differences scheme.[14] The indices i and j are introduced to indicate the axial and circumferential position of a nodal point in the shell. The functional I is replaced by a finite summation through using the Simpson's rule for the integration. The explicit expressions for accelerations at any time step $t=q\Delta t$ may be obtained by minimizing the functional I^q with respect to each of the discrete accelerations as follows:

$$\begin{aligned}\frac{\partial I^q}{\partial\ddot{u}_{ij}^q}&=\frac{\partial I^q}{\partial\ddot{v}_{ij}^q}=\frac{\partial I^q}{I\ddot{w}_{ij}^q}=\frac{\partial I^q}{\partial\ddot{U}^q}\\&=\frac{\partial I^q}{\partial\ddot{V}^q}=\frac{\partial I^q}{\partial\ddot{\phi}^q}=0\end{aligned} \quad (20)$$

It is assumed that at time $t=q\Delta t$, the displacements and velocities have been previously determined at all nodal points of the domain. Then Eq. (20) may be used to determine all the discrete accelerations at time $t=q\Delta t$. Subsequently, the displacements at time $t+\Delta t$ may be obtained by the central difference approximations such as

$$u_{ij}^{q+1}=\ddot{u}_{ij}^q(\Delta t)^2+2u_{ij}^q-u_{ij}^{q-1} \quad (21)$$

Knowing the displacements at $t+\Delta t$, the strain increments that occurred in the time interval $(t+\Delta t-t)$ may be determined by using the central difference scheme. Furthermore, the corresponding stress increments may be determined by the stress-strain relationship provided that the conditions of loading or unloading are evaluated.

The pressure p, is given by Eq. (13), acting on a shell element at time t depends on the position of the wave front relative to the element. During the time interval $(t+\Delta t-t)$, the pressure varies and the wave front moves. Fig. 3 shows six possible situations of the wave front at times $t+\Delta t$ and t relative to an element. In the numerical calculations, an

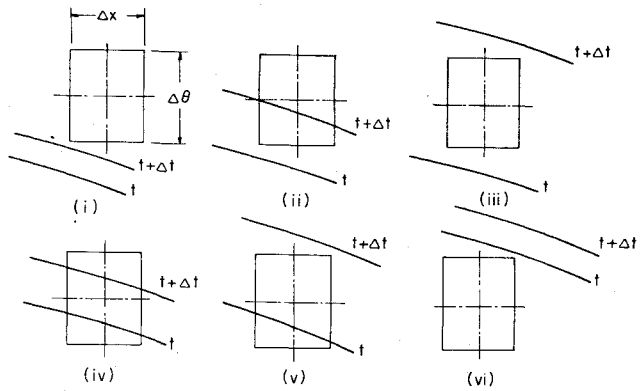

Fig. 3 Various positions of shock fronts at times t and $t+\Delta t$ with respect to an element.

average pressure which produces an equivalent resultant impulse is employed. The average pressure p_a is defined by

$$p_a^{q+1}\Delta x\cdot\Delta\theta\cdot\Delta t=\int_t^{t+\Delta t}\int_{x-\Delta x/2}^{x+\Delta x/2}\int_{\theta-\Delta\theta/2}^{\theta+\Delta\theta/}p(x,\theta,t)\,d\theta dx dt \tag{22}$$

The integral in Eq. (22) is obtained by assuming a timewise and spacewise linear variation of p within the limits and within the area swept by a wave front. The average pressures for the 6 cases shown in Fig. 3 are given approximately as follows:

a) $(p_a)_{ij}^{q+1}=0$

b) $(p_a)_{ij}^{q+1}=p_m\left[\frac{t_2}{\gamma}-1+e^{-t_2/\gamma}\right]$

c) $(p_a)_{ij}^{q+1}=p_m\left[\frac{\Delta t}{\gamma}-e^{-t_2/\gamma}(e^{\Delta t/\gamma}-1)\right]$

d) $(p_a)_{ij}^{q+1}=p_m\left[\frac{\Delta t}{\gamma}-e^{-t_1/\gamma}(1-e^{-\Delta t/\gamma})\right]$

e) $(p_a)_{ij}^{q+1}=p_m\left[\frac{\Delta\tau-t_1}{\gamma}-e^{-(t_2-\Delta\tau)/\gamma}(1-e^{-\Delta t/\gamma})\right]$

f) $(p_a)_{ij}^{q+1}=p_m e^{-t_1/\gamma}(1-e^{-\Delta t/\gamma})(e^{\Delta\tau/\gamma}-1)$ (23)

where

$$t_1=t-\tau(x,\theta-\frac{\Delta\theta}{2})$$

$$t_2=t_1+\Delta t$$

$$\Delta\tau=\frac{1}{C_0}\left[r(x,\theta+\frac{\Delta\theta}{2})-r(x,\theta-\frac{\Delta\theta}{2})\right]$$

$\gamma=\gamma(x,\theta)$, by Eq. (14)

and, for a TNT charge,

$$p_m=\frac{\gamma^2}{\Delta t\Delta\tau}\times 2.16\times 10^4\left[\frac{W^{1/3}}{r(x,\theta)}\right]^{1.13} \tag{24}$$

Knowing the pressure loading, the discrete accelerations at time $t+\Delta t$ may be again determined by Eq. (20). By repeating the foregoing steps for each subsequent time increment, the entire history of deformation of the shell may be obtained.

Numerical Results and Discussion

Numerical results have been obtained by the foregoing approach for the following ring-stiffened cylindrical shells made of steel HY-80 and having the geometric properties shown in Table 1. The shells are initially subjected to a static pressure equivalent to that in water at a depth of 100 ft. They are subjected to shock waves equivalent to that caused by exploding, in water, TNT charges of weights indicated by the shock factor F in Table 1. The shells have the following common dimensions: length $L=152$ in., radius $a=24$ in., width of the ring stiffeners $b=0.4$ in., and width of the end plates $b_E=1.5$ in. The material has a mass density of 0.000733 lb-sec^2/in.^{4} and a Poisson's ratio of 0.3. The uniaxial stress-strain relationship is described in terms of the three parameters in Eq. (12) with E (Young's modulus) $=30.5\times10^6$ psi, $F_{.7}$ (Secant yield stress) $=8.75\times10^4$ psi and γ (shape factor) $=30$.

Table 1 Geometric properties

	a/h	d/h	R/a	N	F
Case 1	80	1.2	4	12	0.4
Case 2	80	1.2	4	12	0.6
Case 3	80	2.4	4	12	0.4
Case 4	100	1.2	4	12	0.4
Case 5	80	1.2	4	6	0.4

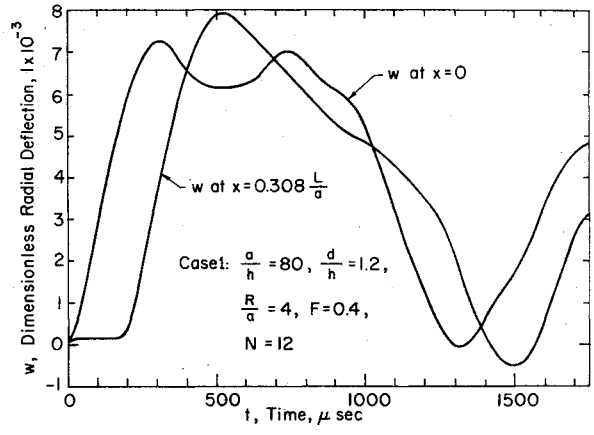

Fig. 4 Radial deflection histories of case 1 at $\theta=0°$.

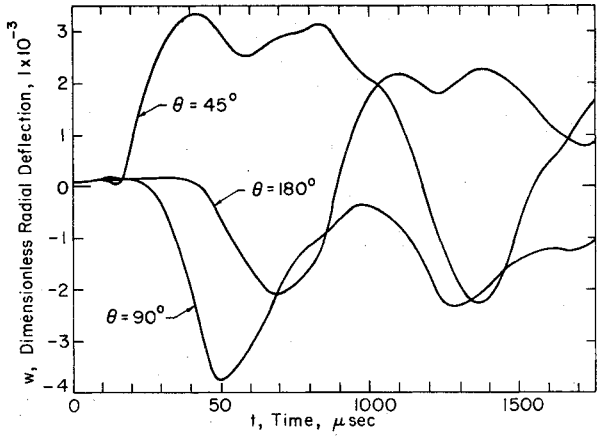

Fig. 5 Radial deflection histories of case 1 at $x=0$.

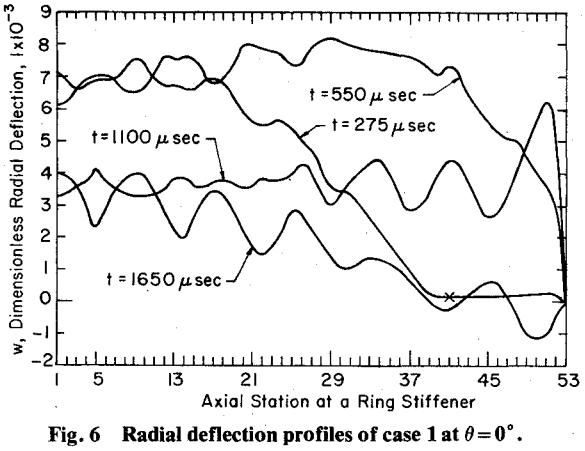

Fig. 6 Radial deflection profiles of case 1 at $\theta=0°$.

In most of the cases, the middle surface of one half of a shell is covered by a network consisting of 53×61 stations, except for case 5 where 57×61 stations are employed. Each shell is replaced by an idealized sandwich shell having five equal thickness layers. The states of stress and deformation of each shell under the hydrostatic pressure prior to the explosion are obtained by an approach given in Ref. 15. The superposed dynamic behavior is determined by the present approach. The time increment in the timewise step-by-step integration

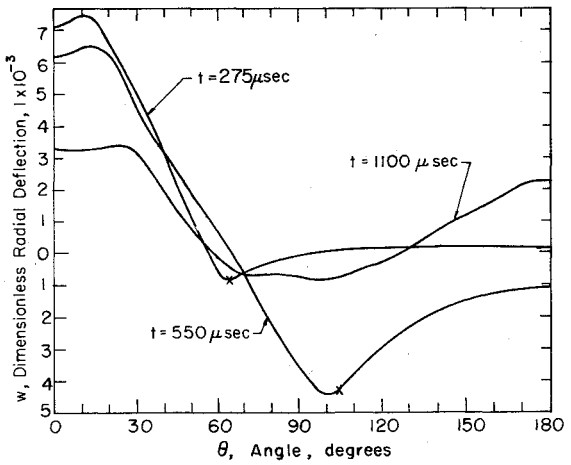

Fig. 7 Radial deflection profiles of case 1 at $x = 0$

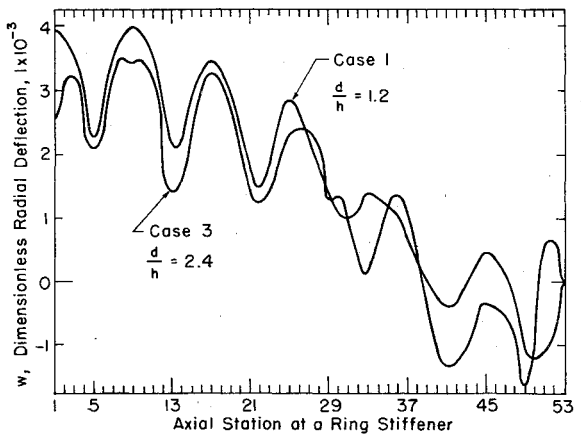

Fig. 10 Comparison of radial deflection profile of case 3 with that of case 1 at $\theta = 0°$ and $t = 1650$ μsec.

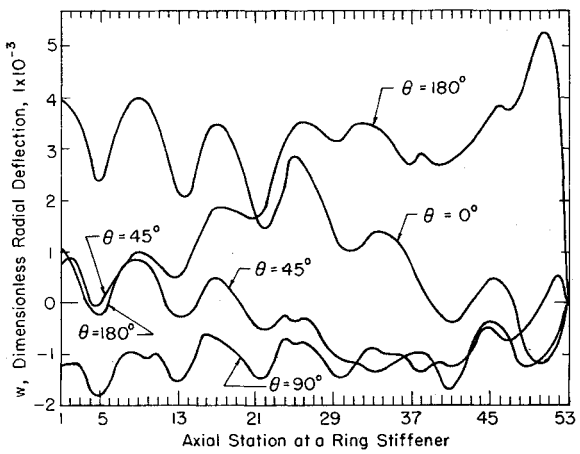

Fig. 8 Radial deflection profiles of case 1 at $t = 1650$ μsec.

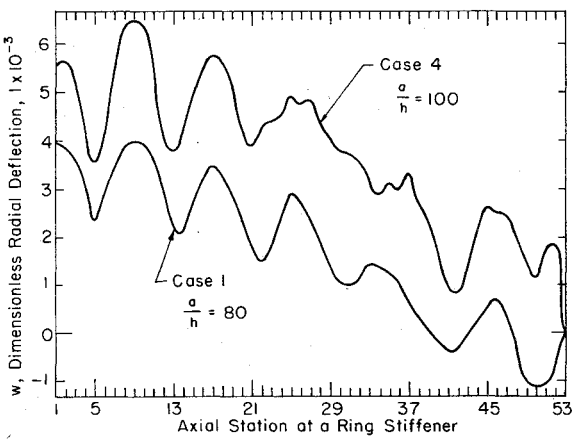

Fig. 11 Comparison of radial deflection profile of case 4 with that of case 1 at $\theta = 0°$ and $t = 1650$μsec.

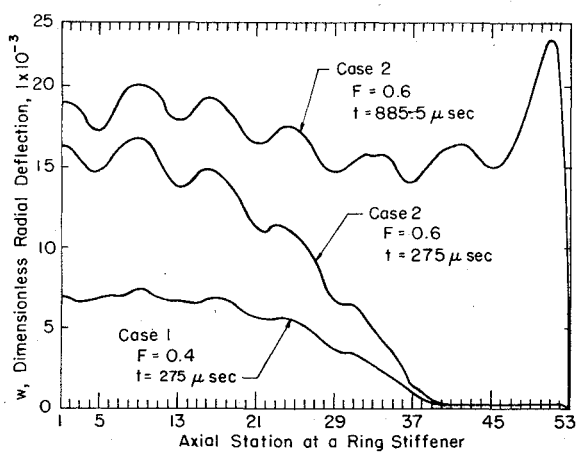

Fig. 9 Comparison of radial deflection profiles of case 2 with that of case 1 at $\theta = 0°$.

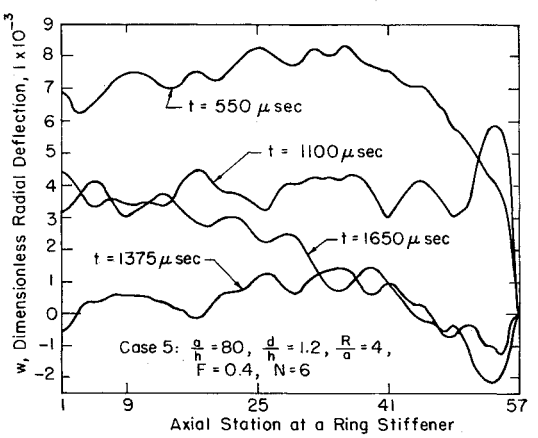

Fig. 12 Radial deflection profiles of case 5 at $\theta = 0°$.

scheme must be sufficiently small in order to assure the numerical stability and meaningful results. The upper bound of the time increment for the numerical stability of the finite-differences method applied to an elastic wave propagation problem is given by[16,17]

$$\Delta t < \Delta x (\rho/E)^{1/2} \tag{25}$$

In the present problem, where plastic as well as elastic wave propagations may occur, a time increment of $\Delta t = 5.5$μsec is employed. The computation by the present approach, for each case, required about 56 min of computing time on an IBM 370-158 computer. The computation was terminated when a maximum strain reached a value of 5% or when the surface pressure acting on the shell diminished.

Figures 4 and 5 give the numerically determined histories of radial deflections at a number of points of the shell in case 1. Figures 6, 7 and 8 show the radial deflection profiles, of case 1, of a number of axial and circumferential sections at various times. In Fig. 6 and the sequel, Axial Station 1 indicates the plane of symmetry with no ring stiffener. The mark x in Figs. 6 and 7 indicates the position of the shock front at a specific time. Figures 5 and 7 show that a region of the shell bulges outward before the arrival of the shock front. The two curves marked by $t = 275$μsec and $t = 550$ μsec in Fig. 7 indicate a

form of strain energy transmission, from that of membrane stresses to that of bending stresses, which may occur in a dynamic buckling process. The phenomenon may be predicted by an analysis which takes the nonlinear goemetric and material effects into account, such as the present one. Figures 6 and 8 show that large curvature changes and consequent plastic yielding of the shell occur at the ring stiffeners and especially near the rigid end plate. The shock front sweeps over the entire shell in a time duration of about 1140 μsec. Figures 6 and 8 show that, after the passage of the shock, the transient vibration of the shell subsides.

Figure 9 gives a comparison of radial deflection profiles of case 2 with that of case 1. In case 2, the shell has a geometry identical to that of case 1, except it is subjected to an explosion of a larger charge. As expected, the amplitudes of the radial deflections in case 2 are more than twice larger than that of case 1 at the corresponding time. At $t=885.5$ μsec the axial strain in the shell near the end plate has a value of more than 5%, which indicates a so-called "hard point failure." The present numerical results agree qualitatively with the experimental results on the hard-point failures of single layer cylinders by Opat and Menkes.[18]

Figure 10 gives a comparison of a radial deflection profile of case 3 with that of case 1. The depth of the ring stiffeners of the shell in case 3 is twice that in case 1, but all the other parameters of the two shells are identical. Figure 10 shows that the average radial deflection of case 3 is slightly less than that of case 1. However, an examination of the deformation histories shows that the maximum axial strains in the shell in case 3 near the ring stiffeners are, in general, more than 50% larger than the corresponding ones in case 1. It indicates that there is no advantage to over stiffen a shell. In either case, the critical strain occurs in the shell near the end plate, or at the hard point.

Figure 11 gives a comparison of a radial deflection profile of case 4 with that of case 1. The shell in case 4 is thinner than that in case 1. Figure 11 shows that the thinner shell is deformed more severely. Figure 12 gives a numer of radial deflection profiles of the shell in case 5, which has 6 ring stiffeners, versus 12 in case 1. The deformation histories indicate that the shell in case 5 withstands the explosion as well as the shell in case 1.

Conclusions

The inelastic response of ring-stiffened cylindrical shells to prescribed time-dependent loads may be determined by the incremental finite-differences method based on the absolute minimum principle employed herein. The effects of a number of geometric parameters on the resistance of ring-stiffened cylindrical shells to pressure shock waves are illustrated by the numerical results obtained by the method. However, to solve the problem more realistically, further theoretical and experimental studies on the complex nature of nonlinear fluid-solid interactions are required.

References

[1] Cole, R. H., *Underwater Explosions,* Princeton University Press, Princeton, N.J., 1948.

[2] Carrier, G. F., "The Interaction of an Acoustic Wave and an Elastic Cylindrical Shell," Contract N7 ONR-35810, Tech. Rept. 4, Brown University, Providence, R.I., Oct. 1951.

[3] Mindlin, R. D. and Bleich, H. H., "Response of an Elastic Cylindrical Shell to a Transverse Step Shock Wave," *Journal of Applied Mechanics,* Vol. 20, No. 2, 1953, pp. 189-195.

[4] Baron, M. L., "The Response of a Cylindrical Shell to a Transverse Shock Wave," *Proceedings Second U. S. National Congress of Applied Mechanics,* University of Michigan, Ann Arbor, Mich., 1954, pp. 201-212.

[5] Haywood, R. W., "Response of an Elastic Cylindrical Shell to a Pressure Pulse," *Quarterly Journal of Mechanics and Applied Mathematics,* Vol. 11, Pt. 2, 1958, pp. 129-141.

[6] Herrmann G. and Russell, J. E., "Forced Motions of Plates and Shells Surrounded by an Acoustic Fluid," *Proceedings, Symposium on the Theory of Shells* to honor Lloyd Hamilton Donnell, University of Houston, Houston, Tex., 1967.

[7] Herman, H. and Klosner, J. M., "Transient Response of a Periodically Supported Cylindrical Shell Immersed in a Fluid Medium," *Journal of Applied Mechanics,* Vol. 32, No. 3, Series E, 1965, pp. 562-568.

[8] Berglund, J. W. and Klosner, J. M., "Interaction of a Ring-Reinforced Shell and a Fluid Medium," *Journal of Applied Mechanics,* Vol. 32, No. 3, Ser. E, 1965, pp. 562-568.

[9] Crouzet-Pascal, J. and Garnet, H., "Response of a Ring-Reinforced Cylindrical Shell, Immersed in a Fluid Medium, to an Axisymmetric Step Pulse," *Journal of Applied Mechanics,* Vol. 39, No. 2, June 1972, pp. 521-526.

[10] Klosner, J. M., "Inadequacies of Piston Theory in Fluid-Shell Interactions," *Journal of Engineering Mechanics Division,* Proceedings of A.S.C.E., 1970, pp. 143-159.

[11] Lee, L.H.N. and Ni, C.M., "A Minimum Principle in Dynamics of Elastic-Plastic Continua at Finite Deformation," *Archives of Mechanics,* Vol. 25, No. 3, March 1973, pp. 457-468.

[12] Pars, L. A., *A Treatise on Analytical Dynamics,* Heinemann, London, pp. 12, 40, 42, 200-201, 1965.

[13] Ramberg, W. and Osgood, W. R., "Description of Stress-Strain Curves by Three Parameters," TN 902, 1943, U. S. National Advisory Committee for Aeronautics, Washington, D. C.

[14] Lee, L.H.N. and Horng, J.T., "Inelastic Response of Ring-Stiffened Cylindrical Shells to External Pressure Shock Waves," Technical Rept. UND-75-1, Mar. 1975, Deep Ocean Engineering, University of Notre Dame, Notre Dame, Ind.

[15] Lee, L.H.N., "Inelastic Asymmetric Buckling of Ring-Stiffened Cylindrical Shells under External Pressure," *AIAA Journal,* Vol. 12, Aug. 1974, pp. 1051-1056.

[16] Witmer, E. A., Balmer, H. A., Leech, J. W. and Piam, T. H. H., "Large Dynamic Deformations of Beams, Rings, Plates and Shells," *AIAA Journal,* Vol. 1, Dec. 1963, pp. 1848-1856.

[17] Ni, C. M. and Lee, L.H.N., "Dynamic Behavior of Inelastic Cylindrical Shells at Finite Deformation," *International Journal of Nonlinear Mechanics,* Vol. 9, No. 1, Jan. 1974, pp. 193-207.

[18] Opat, H. J. and Menkes, S. B., "Hard Point Failure in Relationship to Lethality, Phase II: Experimental Results for Single Layer Cylinders," Technical Rept. 4738, Picatinny Arsenal, Dover, N.J., Nov. 1974.